

## Unidentified gamma-ray sources: hunting $\gamma$ -ray blazars

F. Massaro<sup>1</sup>, R. D'Abrusco<sup>2</sup>, G. Tosti<sup>3,4</sup>, M. Ajello<sup>1</sup>, A. Paggi<sup>2</sup>, D. Gasparrini<sup>5</sup>.

### ABSTRACT

One of the main scientific objectives of the ongoing *Fermi* mission is unveiling the nature of the unidentified  $\gamma$ -ray sources (UGSs). Despite the large improvements of *Fermi* in the localization of  $\gamma$ -ray sources with respect to the past  $\gamma$ -ray missions, about one third of the *Fermi*-detected objects are still not associated to low energy counterparts. Recently, using the Wide-field Infrared Survey Explorer (*WISE*) survey, we discovered that blazars, the rarest class of Active Galactic Nuclei and the largest population of  $\gamma$ -ray sources, can be recognized and separated from other extragalactic sources on the basis of their infrared (IR) colors. Based on this result, we designed an association method for the  $\gamma$ -ray sources to recognize if there is a blazar candidate within the positional uncertainty region of a generic  $\gamma$ -ray source. With this new IR diagnostic tool, we searched for  $\gamma$ -ray blazar candidates associated to the UGS sample of the second *Fermi*  $\gamma$ -ray catalog (2FGL). We found that our method associates at least one  $\gamma$ -ray blazar candidate as a counterpart each of 156 out of 313 UGSs analyzed. These new low-energy candidates have the same IR properties as the blazars associated to  $\gamma$ -ray sources in the 2FGL catalog.

*Subject headings:* galaxies: active - galaxies: BL Lacertae objects - radiation mechanisms: non-thermal

---

<sup>1</sup>SLAC National Laboratory and Kavli Institute for Particle Astrophysics and Cosmology, 2575 Sand Hill Road, Menlo Park, CA 94025

<sup>2</sup>Harvard - Smithsonian Astrophysical Observatory, 60 Garden Street, Cambridge, MA 02138

<sup>3</sup>Dipartimento di Fisica, Università degli Studi di Perugia, 06123 Perugia, Italy

<sup>4</sup>Istituto Nazionale di Fisica Nucleare, Sezione di Perugia, 06123 Perugia, Italy

<sup>5</sup>ASI Science Data Center, ESRIN, I-00044 Frascati, Italy

## 1. Introduction

More than half of the  $\gamma$ -ray sources detected by *Compton* Gamma-Ray Observatory (CGRO), and present in the third EGRET (3EG) catalog were not associated with known counterparts seen at low energies (Hartman et al. 1999). Whatever the nature of the unidentified  $\gamma$ -ray sources (UGSs), these objects could provide a significant contribution to the isotropic gamma-ray background (IGRB) (e.g., Abdo et al. 2010a). Solving the puzzle of the origin of the UGSs, together with a better knowledge of other IGRB contributions estimated from known sources, is crucial also to constrain exotic high-energy physics phenomena, such as dark matter signatures, or new classes of sources.

With the advent of the *Fermi* mission the localization of  $\gamma$ -ray sources has significantly improved with respect to the past  $\gamma$ -ray missions, thus simplifying the task of finding statistically probably counterparts at lower energies. New association methods also have been developed and applied, so that the number of UGSs has significantly decreased with respect to the 3EG catalog (Hartman et al. 1999); however, according to the second *Fermi*  $\gamma$ -ray catalog (2FGL), about one third of detected gamma-ray sources in the energy range above 100 MeV is still unassociated (Abdo et al. 2011). It is worth noting that the most commonly detected sources in the  $\gamma$ -ray sky, since the epoch of CGRO, are blazars, one of the most enigmatic classes of Active Galactic Nuclei (AGNs) (e.g., Hartman et al. 1999). Within the 2FGL, there are 576 UGSs out of a total number of 1873 sources detected, while among the 1297 associated sources,  $\sim 1000$  have been associated with AGNs (Abdo et al. 2011; Ackermann et al. 2011a).

Blazar emission extends over the whole electromagnetic spectrum and is generally interpreted as non-thermal radiation arising from particles accelerated in relativistic jets closely aligned to the line of sight (Blandford & Rees 1978). They come in two flavors: the BL Lac objects, with featureless optical spectra or only with absorption lines of galactic origin and weak and narrower emission lines, and the Flat Spectrum Radio Quasars, with a optical spectra showing broad emission lines. In the following, we indicate the former as BZBs and the latter as BZQs, respectively, according to the ROMA-BZCAT<sup>1</sup> nomenclature (Massaro et al. 2009; Massaro et al. 2010; Massaro et al. 2011a).

The first step to improve our knowledge on the origin of the UGSs and of their associations with low-energy counterparts, is to recognize those that could have a blazar within their  $\gamma$ -ray positional uncertainty regions.

Recently, we developed a procedure to identify blazars using their infrared (IR) colors

---

<sup>1</sup><http://www.asdc.asi.it/bzcat/>

within the preliminary data release of the Wide-field Infrared Survey Explorer (*WISE*) survey (Wright et al. 2010)<sup>2</sup>. In particular, we discovered that the IR color space distribution of the extragalactic sources dominated by non-thermal emission, as blazars, can be used to distinguish such sources from other classes of galaxies and/or AGNs and/or galactic sources (Massaro et al. 2011b, hereinafter Paper I). We also found that  $\gamma$ -ray emitting blazar delineate a narrow, distinct region of the IR color-color plots, denominated as the *WISE* Gamma-ray blazar Strip (*WGS*) (D’Abrusco et al. 2012, hereinafter Paper II). There is a peculiar correspondence between the IR and  $\gamma$ -ray spectral properties of the blazars detected in the 2FGL (Paper II). Then, on the basis of our previous investigation of these IR- $\gamma$ -ray properties of blazars, we built a parametrization of the *WGS* to evaluate how many AGNs of Uncertain type (AGUs) have a counterpart associated with a  $\gamma$ -ray blazar candidate in the 2FGL (Massaro et al. 2012a, hereinafter Paper III).

In this paper, we present a new association method based on the IR colors of the  $\gamma$ -ray emitting blazars and the *WGS* parametrization. Then we apply this new association procedure to search for  $\gamma$ -ray blazar candidates within the  $\gamma$ -ray positional error regions of the UGSs. One of the main advantages of our method is that it reduces the number of potential counterparts for the UGSs and provides their positions with arcsec resolution, thus restricting the search regions for future followup observations necessary to confirm their blazar nature. Unfortunately, only a restricted number of UGSs falls within the portion of the sky currently covered by the IR observations of the *WISE* Preliminary Data Release corresponding to  $\sim 57\%$  of the whole sky. Then, when the *WISE* survey will be completely released in March 2012<sup>3</sup>, it will be possible to apply the method to the whole sky, even in regions not covered at radio, optical and X-ray frequencies, where the other methods for establishing counterpart associations for the 2FGL cannot be used.

This paper is organized as follows: in Section 2 we describe the samples used in our investigation; in Section 3 we illustrate the new association method; then, in Section 4 we apply the new association technique to the UGSs and describe the subset of sources that has been associated with  $\gamma$ -ray blazar candidates. In Section 5, we also compare our results with those found adopting different statistical approaches for a subsample of UGSs. Finally, conclusions are presented in Section 6.

---

<sup>2</sup><http://wise2.ipac.caltech.edu/docs/release/prelim/>

<sup>3</sup><http://wise2.ipac.caltech.edu/docs/release/allsky/>

## 2. The sample selection

To build our association procedure we considered a sample of blazars selected from the combination of the ROMA-BZCAT (Massaro et al. 2009; Massaro et al. 2010) and the 2FGL (Abdo et al. 2011), as described and used in Paper II and used in Paper III to parametrize the *WGS*, denoted the 2FB sample. It contains 284  $\gamma$ -ray blazars (135 BZBs and 149 BZQs) that have optical and radio counterparts as reported in the ROMA-BZCAT, and also having a *WISE* counterpart within 2.4 " radius (see Paper I and III). The blazars in the 2FB sample are detected by *WISE* with a signal to noise ratio higher than 7 in at least one band and do not have any upper limits in all the *WISE* bands. We excluded from our analysis all the blazars with a *Fermi* analysis flag, according to the 2FGL and the 2LAC (Abdo et al. 2011; Ackermann et al. 2011a). The blazars of uncertain type (BZUs) have been excluded from our analysis, while the BL Lac candidates have been considered as BZBs. More details on the 2FB sample and the source selections are given in Papers II and III.

Then, we applied our association procedure to the sample of the UGS defined as follows. The number of UGSs in the 2FGL is 576, but only 410 of these  $\gamma$ -ray sources lie in the region of the sky available in the *WISE* Preliminary Data Release. These sources can be analyzed according to our method based on the IR *WISE* colors. We adopted a more conservative selection restricting our sample to 313 UGSs out of 410, excluding sources with a *Fermi* analysis flag, since these sources might not be real and/or could be affected by analysis artifacts (see e.g. Abdo et al. 2011, for more details).

## 3. The *WGS* association method

In Paper III, working on the AGUs, we built the *WGS* parametrization to verify if the low-energy counterparts of the AGUs, associated in 2FGL, is consistent with the *WGS*, so being a  $\gamma$ -ray blazar candidate. With respect to the previous analysis, the following proposed association procedure aims at providing new  $\gamma$ -ray blazar candidates, possible counterparts of the UGSs, that lie within their  $\gamma$ -ray positional uncertainty regions, on the basis of our previous results on the IR- $\gamma$ -ray blazar properties. In this Section, we report the basic details of our *WGS* parametrization together with the definition of different classes of  $\gamma$ -ray blazar candidates. Then we describe our new association procedure.

### 3.1. The *WGS* parametrization

In Paper II, we found that  $\gamma$ -ray emitting blazars (i.e., those in the 2FB sample) cover a narrow region in the 3D color space built with the *WISE* magnitudes delineating the so-called *WISE* Gamma-ray blazar Strip (*WGS*).

In Paper III, using the 2FB sample, we presented the parametrization of the *WGS* based on the *strip parameter*  $s$ . This parameter, ranging between 0 and 1, provides a measure of the distance between the *WGS* and the location of a *WISE* source in the three dimensional IR color parameter space. For example, sources with high values of  $s$  (e.g.,  $\geq 0.50$ ) are consistent with the *WGS*. We also distinguished between *WISE* sources that lie in the subregion of the *WGS* occupied by the BZBs and BZQs using the  $s_b$  and  $s_q$  parameters separately (Paper III).

The IR color space has been built using the archival data available in the 2011 *WISE* Preliminary Data Release, in four different bands centered at 3.4, 4.6, 12, and 22  $\mu\text{m}$  with an angular resolution of 6.1, 6.4, 6.5 & 12.0'', respectively and achieving  $5\sigma$  point source sensitivities of 0.08, 0.11, 1 and 6 mJy. In addition, the absolute (radial) differences between *WISE* source-peaks and “true” astrometric positions anywhere on the sky are no larger than  $\sim 0.50$ , 0.26, 0.26, and 1.4'' in the four *WISE* bands, respectively (Cutri et al. 2011)<sup>4</sup>.

### 3.2. $\gamma$ -ray blazar candidate definition

Based on the  $s_b$  and  $s_q$  distributions of all *WISE* sources in different random regions of the sky, at both high and low Galactic latitudes (Paper III), the critical threshold of the  $s$  parameters, used to define the above classes, have been arbitrarily determined on the basis of the following considerations:

- class A: *WISE* sources with  $0.24 < s_b < 1.00$  and  $0.38 < s_q < 1.00$ ;
- class B: *WISE* sources with  $0.24 < s_b < 1.00$  or  $0.38 < s_q < 1.00$ ;
- class C: *WISE* sources with  $0.10 < s_b < 0.24$  and  $0.14 < s_q < 0.38$ .

All the *WISE* sources with  $s_b < 0.10$  or  $s_q < 0.14$  are considered *outliers* of the *WGS* and, for this reason, discarded. All the above thresholds are then used to select the *WISE* sources that are associated to the UGSs and that can be considered potential  $\gamma$ -ray blazar candidates.

---

<sup>4</sup><http://wise2.ipac.caltech.edu/docs/release/prelim/expsup/sec2.3g.html>

The above choice of threshold have been adopted for the analysis of the  $\gamma$ -ray blazar content within the AGUs (Paper III). From the distributions of the  $s_b$  and  $s_q$  parameters for the generic IR *WISE* sources, we note that 99.9% of them have  $s_b < 0.24$  and  $s_q < 0.38$ . Then, for the BZBs in the 2FB sample only 6 sources out of 135 have  $s_b < 0.24$ , and in the case of the BZQs only 33 sources out of 149 show  $s_q$  values lower than 0.38. We also note that 99.0% of the generic IR *WISE* sources have  $s_b < 0.10$  and only 2 BZBs are below this value, while 97.2% of the generic IR *WISE* sources together with only 5 BZQs out of 149 have  $s_q < 0.14$ .

The *WISE* objects of class A are the most probable blazar counterpart of the unidentified  $\gamma$ -ray sources, because their WISE colors are more consistent with the WGS in both the BZBs and BZQs subregions than the colors of sources of class B or C. Based on the distributions of the  $s_b$  and  $s_q$  parameters for *WISE* sources in random region of the sky, the sources of class A are, as expected, rarer than the sources belonging to the other two classes (see Section 4 for more details).

### 3.3. The association procedure

For each unidentified  $\gamma$ -ray source we defined the *searching region* (SR) corresponding to a circular region of radius  $R = \theta_{999}$ , centered on the position given in the 2FGL, where  $\theta_{999}$  is the major axis of the elliptical source location region corresponding to the 99.9% level of confidence. In addition, we also considered a *region of comparison* (ROC) defined as a circular region of the same radius  $R$ , but lying at  $2.5\sqrt{2}$  deg angular distance from the 2FGL position. A schematic view of the locations of the SR and the ROC is shown in Figure 1.

Successively, for every unassociated gamma-ray source in the 2FGL catalog, we ranked all the *WISE* sources within its SR on the basis of the classification described above and we selected as  $\gamma$ -ray blazar candidates the positionally closest sources with the highest class. In our analysis we considered only sources of the *WISE* preliminary catalog detected in all the four *WISE* bands, without any upper limit.

The ROCs are used to assess the association confidence that a *WISE* source in a random region in the sky, where no  $\gamma$ -ray source is located, has IR colors compatible with the WGS. To provide an estimate of the association confidence, we considered the distribution of the strip parameters  $s_b$  and  $s_q$  for all the *WISE* sources within each ROC associated to an UGS. For these *WISE* sources we estimated the confidence  $\pi$  that a generic *WISE* source belongs to the same class as the  $\gamma$ -ray blazar candidate selected within the SR. Thus the  $\pi$  value will be expressed as the ratio between the number of *WISE* sources of a particular class and the

total number of *WISE* sources that lie in the ROC.

### 3.4. Testing the association method with blazars

We performed a test to evaluate the completeness of our association method searching for the  $\gamma$ -ray blazar candidates that are potential counterparts of the 2FB sample, and verifying whether our procedure correctly finds the same associations as in the 2FB sample.

Assuming that the 284 blazars in the 2FB sample have been associated to the real low-energy counterparts, we run our association procedure considering the IR colors for all the *WISE* sources within the SRs for all these sources. We found that for the population of BZBs, consisting of 135 BL Lacs, our association procedure is able to recognize 123 sources as the 2FGL, 62 of class A, and 61 of class B. Within the remaining 12 BZBs, 3 objects are associated to *WISE* sources of higher class than the original 2FGL associated sources, while for 9 sources we only found outliers of the *WGS* within their SRs.

For the BZQs, our method finds the same associations as in the 2FGL catalog for 124 of the sources, with 85 sources classified as class A, 32 classified as class B and 7 as class C. For the remaining 25 sources, we found 11 outliers and 14  $\gamma$ -ray sources associated to a *WISE* source with higher classes.

Our procedure re-associates 247 out of 284  $\gamma$ -ray blazars of the 2FB sample in agreement with the 2FGL analysis, with a completeness of 87.0% (91.0% for the BZBs and 83.0% for the BZQs). We found that 7.1% are outliers of the *WGS*, but this number can be expected because the *WGS* parametrization was built to require at least 90% of the 2FB sources inside each 2-dimensional *WGS* projection (see Paper III for more details).

It is interesting to note that 17 out of 284  $\gamma$ -ray sources in the 2FGL have a “better”, on the basis of our method,  $\gamma$ -ray blazar candidate within the SR. These associations need to be verified with followup observations, as for example in the X-rays, and a deeper analysis to check their reliability relative to the 2FGL association method will be performed in a forthcoming paper (Massaro et al. 2012b).

## 4. Results

The application of our association procedure to the 313 UGSs selected from the 2FGL (see Section 2 for more details), led to the associations of 156 UGSs with a low-energy candidate  $\gamma$ -ray blazar counterpart within their SRs. According to our criteria (see Section 3.2),

these 156 new associations consist of 44 sources of class A, 74 of class B and 38 of class C. Thus our procedure finds associations with likely  $\gamma$ -ray blazar candidates for 49.8% of the UGSs analyzed. We also list of all the  $\gamma$ -ray blazar candidates with lower class for each UGSs, if more than one is present within the SRs. Among these 156 new associations, for 86 sources, 12 of class A, 43 of class B and 31 of class C, have only a single  $\gamma$ -ray blazar candidate within the SR. In Figure 2 we show the *WISE* colors of the 156  $\gamma$ -ray blazar candidates in comparison with those of the blazars in the 2FB sample for the [3.4]-[4.6]-[12]  $\mu\text{m}$  2D projection of the *WGS*.

By restricting our sample of UGSs only to those at high Galactic latitudes, i.e.  $|b| > 15^\circ$ , we found a  $\gamma$ -ray blazar candidate for 72 UGSs, 16 of class A, 29 of class B and 27 of class C; where for 34 out of these 74, the low energy counterpart associated with our method is univocal. In Figure 3, we shown the distribution of the Galactic latitude (i.e.,  $\sin b$ ) for all the UGSs analyzed in comparison with those 156 associated by our method. At high Galactic latitude, the method seems to be less efficient given the ratio between the number of UGSs analyzed and those associated. This could be due to the non uniform exposure of the archival *WISE* observations in the *WISE* Preliminary Data Release<sup>5</sup>, and will be re-analyzed once the whole *WISE* archive will be available. In addition, we note that our association method could be more efficient at low Galactic latitudes where the blazar catalogs, as the ROMA-BZCAT, are less complete (Massaro et al. 2009).

We also remark that within the 313 regions of comparison chosen for the UGSs there are 55195 *WISE* sources, but only 49 of class A, 213 of class B and 129 of class C, all of them detected in all four *WISE* bands and with a signal to noise ratio higher than seven in at least one band, as the blazars in the 2FB sample. The distributions of the  $s_b$  and  $s_q$  parameters for all the 55195 *WISE* sources within the 313 ROCs are shown in Figure 4. A blind search of all the possible  $\gamma$ -ray blazar candidates in the *WISE* archive on the basis of the *WGS* properties will be performed once it will be completely available (Massaro et al. 2012b). However, the  $s_b$  and  $s_q$  distributions reported in Figure 4 strongly suggest that the density of *WISE* blazar candidates is low over the sky.

In Table 1 we show three cases of *WISE* sources that have been associated with our procedure to three UGSs. We report both the  $s_b$  and  $s_q$  values, the *WGS* class and the association confidence  $\pi$ . In this example, the source 2FGL J0038.8+6259 is associated to one *WISE* source of a class A, J003818.70+630605.0, that has been selected as a single  $\gamma$ -ray blazar candidate out of 791 *WISE* sources within its SR. The corresponding association confidence  $\pi$ , expressed in terms of number of sources with an higher  $s_b$  or  $s_q$  values than

---

<sup>5</sup>[http://wise2.ipac.caltech.edu/docs/release/prelim/figures/prelim\\_3x3-w1-equ.jpg](http://wise2.ipac.caltech.edu/docs/release/prelim/figures/prelim_3x3-w1-equ.jpg)



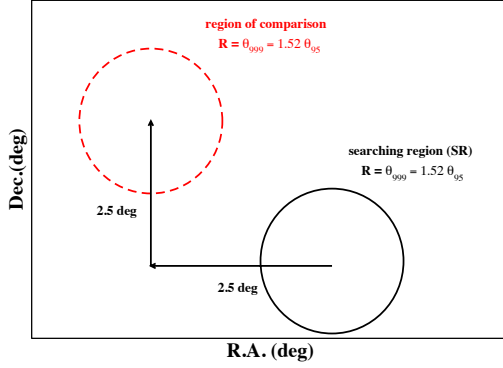


Fig. 1.— The position of the region of comparison (ROC) for a generic *Fermi* source, with respect to the searching region (SR) centered on the position reported in the 2FGL catalog. The radius of both regions is  $R = \theta_{999}$  and they are separated by  $2.5\sqrt{2}$  deg of distance.

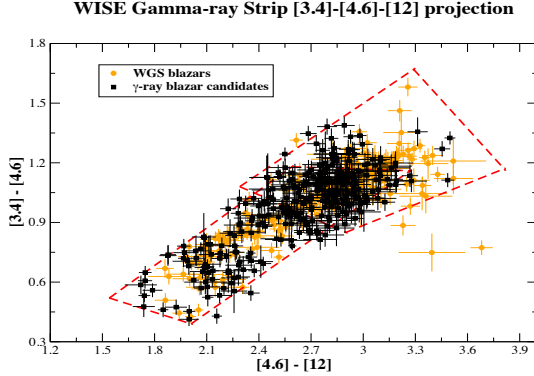


Fig. 2.— The  $[3.4]-[4.6]-[12]$   $\mu\text{m}$  2D projection of the *WGS* is shown. Red dashed lines show the boundaries of the *WGS* used in our analysis (see Paper III for more details). The orange background filled circles are the blazars associated with the 2FGL constituting the 2FB sample while the black filled circles indicate the 156  $\gamma$ -ray blazars that have been associated by our procedure.

J003818.70+630605.0 within the region of comparison and estimated considering 830 *WISE* sources, is 2/830.

Similarly, the source 2FGL J0616.6+2425 has been associated to the *WISE* source J061609.79+241911.0, that belongs to class B with a low association confidence estimated on 5465 *WISE* sources in the region of comparison. The 2FGL source 2FGL J0312.8+2013 has a *WISE* class C source associated following our procedure, with a lower confidence of finding a similar source in a region of comparison where there are 512 *WISE* sources.

Within the 313 UGS analyzed there are 14 sources that have a variability index (Abdo et al. 2011) higher than the value of 41.6 corresponding to the 99% of confidence that the source is variable. It is worth noting that 13 out of these 14 variable UGSs have been successfully associated here with a  $\gamma$ -ray blazar candidate, strongly supporting the blazar nature.

The entire list of the UGSs analyzed can be found in Table 2. For each UGS, we report all the  $\gamma$ -ray blazar candidates with their IR colors (i.e.,  $c_{12} = [3.4]-[4.6] \mu\text{m}$ ,  $c_{23} = [4.6]-[12] \mu\text{m}$  and  $c_{34} = [12]-[22] \mu\text{m}$ , together with their errors,  $\sigma_{12}$ ,  $\sigma_{23}$ ,  $\sigma_{34}$ , respectively), the distances in arc seconds between the  $\gamma$ -ray position and the selected *WISE* source, the  $s_b$  and  $s_q$  values, the class and the association confidence  $\pi$  that there is a *WISE* source of the same class within the ROC (see Section 3.2).

In addition, we found that there are 157 unidentified  $\gamma$ -ray sources that do not have clear  $\gamma$ -ray blazar counterpart within their SRs and are classified as outliers of the *WGS*. The lack of association for these sources could be due to a lower accuracy of the  $\gamma$ -ray position that might occur close to the Galactic plane or to the systematic uncertainties of the diffuse emission model used in the 2FGL analysis. The whole UGS sample will be reconsidered for associations with  $\gamma$ -ray blazar candidates when the all-sky *WISE* survey will be available.

Assuming that all the 2FB blazar associations are correct, on the basis of our test (see Section 3.4), we can argue that within our sample we would expect about 41 ( $\sim 13.0\%$ ) not recognized low-energy counterparts, for a total of 197  $\gamma$ -ray blazar candidates within the 313 UGSs analyzed.

Finally, it is worth stressing that our association procedure provides also interesting information on the sources that do not have a  $\gamma$ -ray blazar candidates in the SR. The absence

Table 1: An example of three UGS associations.

2FGL name	Sources in SR	<i>WISE</i> name	$s_b$	$s_q$	class	$\pi$
J0038.8+6259	791	J003818.70+630605.2	0.89	0.99	A	2/830
J0616.6+2425	6021	J061623.95+241809.2	—	0.57	B	1/5465
J0312.8+2013	453	J031223.00+200749.5	0.19	0.15	C	1/512

of  $\gamma$ -ray blazar candidates selected according to our association procedure could direct to better use the follow-up resources for identifying other  $\gamma$ -ray source candidates. For example in the case of the unidentified  $\gamma$ -ray source: 2FGL J1446.8–4701 within the 1604 *WISE* sources that lie in its SR, we did not find any  $\gamma$ -ray blazar candidates. This source has been recently identified with the pulsar PSR 1446-4701 (see Public List of LAT-Detected Gamma-Ray Pulsars) <sup>6</sup>.

## 5. Comparison with other methods

We note that among the 313 UGSs analyzed, there are 70 sources that were also unidentified according to the investigation performed in the first Fermi  $\gamma$ -ray catalog (1FGL), and 48 of them have been associated with a  $\gamma$ -ray blazar candidates in our analysis. In particular, a recent analysis of the 1FGL unidentified  $\gamma$ -ray sources has been carried out using two different statistical approaches: the Classification Tree and the Logistic regression analyses (see Ackermann et al. 2011b, and references therein).

For 44 out of the 48 UGSs, that have been analyzed on the basis of the above statistical methods, it is also possible to perform a comparison with our results to verify if the 2FGL sources that we associated to a  $\gamma$ -ray blazar candidates have been also classified as AGNs following the Ackermann et al. (2011b) procedures. By comparing the results of our association method with those in Ackermann et al. (2011b), we found that 27 out of 44 UGSs that we associate to a  $\gamma$ -ray blazar candidate are also classified as AGNs, all of them with a probability higher than 71% and 18 of them higher than 80%. Among the remaining 17 out of 44 sources, 7 have been classified as pulsars, with a very low probability with respect to the whole sample; in particular, 3 of these pulsar candidates are classified with a probability lower than 41% and all of them lower than 71%, making these classifications less reliable than those of the AGNs. The last 10 UGSs did not have a classification in Ackermann et al. (2011b). Consequently, we emphasize that our results are in good agreement with the classification suggested previously by Ackermann et al. (2011b) consistent with the  $\gamma$ -ray blazar nature of the *WISE* candidates proposed in our analysis.

---

<sup>6</sup><https://confluence.slac.stanford.edu/display/GLAMCOG/Public+List+of+LAT-Detected+Gamma-Ray+Pulsars>

## 6. Summary and Conclusions

Recently, we discovered that blazars have peculiar mid-IR colors with respect to other galactic sources or different classes of AGNs. In particular, we found that within the 3-dimensional IR parameter space they delineate a distinct, well-defined, region known as *WISE* Blazar Strip (Paper I). Moreover, this distinction, mostly due to the non-thermal emission that dominates the IR radiation of blazars, appears to be more evident when considering those blazars selected on the basis of their  $\gamma$ -ray properties (Paper II) so defining the *WISE* Gamma-ray blazar Strip (*WGS*). Then, in Paper III, we built the *WGS* parametrization to test the consistency of the low energy counterpart of the AGUs, associated in 2FGL with the *WGS*.

On the basis of these results, in the present work, we developed a new association method to search for blazar counterparts of  $\gamma$ -ray sources and we applied this method to the blazars of the 2FGL sample. We also provide new  $\gamma$ -ray blazar candidates, potential counterparts of the UGSs, that lie within their  $\gamma$ -ray positional error region, having the same mid-IR colors as the  $\gamma$ -ray blazars already associated. We also tested our new procedure *a posteriori* trying to re-associate all the blazars in the 2FB sample and we found that our results are in good agreement with different association procedures.

The application of our association procedure to the UGSs has led to the selection of possible blazar counterparts for 156 of 313 UGSs analyzed.

As also noted in Section 4, our association procedure provides also interesting information on the sources that do not have a  $\gamma$ -ray blazar candidates in the SRs as the case of the unidentified  $\gamma$ -ray source: 2FGL J1446.8–4701, recently identified with the pulsar PSR 1446-4701.

Several developments will be considered to improve our association procedure, such as taking into account not only the IR colors, correspondent to flux ratios, but also the IR fluxes as well as the IR- $\gamma$ -ray spectral index correlation (Paper II) and the sky distribution of the  $\gamma$ -ray blazar candidates, once the whole *WISE* data archive will be released. Then, it will be also possible to calibrate our association procedure choosing the different thresholds for the  $s$  parameters at different Galactic latitudes to take into account of the *WISE* background.

Moreover, our association method is complementary to those adopted in the 2FGL catalog analysis, because it is based on different multifrequency information. For this reason, these methods could be in principle combined to increase the fraction of associated UGSs and the efficiency of the association. Further developments of this new association method will be investigated in a forthcoming paper (Massaro et al. 2012b).

We thank the anonymous referee for the his/her comments. F. Massaro is grateful S. Digel for their fruitful discussions for all the comments helpful toward improving our presentation. We also thank to A. Cavaliere, D. Harris, J. Grindlay, J. Knodlseder, P. Giommi, N. Omodei, H. Smith and D. Thompson for their suggestions. The work at SAO and at Stanford University is supported in part by the NASA grant NNX10AD50G, NNX09ZDA001N and NNX10AD68G. R. D’Abrusco gratefully acknowledges the financial support of the US Virtual Astronomical Observatory, which is sponsored by the National Science Foundation and the National Aeronautics and Space Administration. F. Massaro acknowledges the Fondazione Angelo Della Riccia for the grant awarded him to support his research at SAO during 2011 and the Foundation BLANCEFLOR Boncompagni-Ludovisi, n’ee Bildt for the grant awarded him in 2010 to support his research. TOPCAT<sup>7</sup> (Taylor 2005) was used extensively in this work for the preparation and manipulation of the tabular data. Part of this work is based on archival data, software or on-line services provided by the ASI Science Data Center. This publication makes use of data products from the Wide-field Infrared Survey Explorer, which is a joint project of the University of California, Los Angeles, and the Jet Propulsion Laboratory/California Institute of Technology, funded by the National Aeronautics and Space Administration.

## REFERENCES

- Abdo, A. A. et al. 2010a ApJ, 720, 435
- Abdo, A. A. et al. 2010b ApJS 188 405
- Abdo, A. A. et al. ApJS submitted <http://arxiv.org/abs/1108.1435>
- Ackermann, M. et al. 2011a ApJ, 743, 171
- Ackermann, M. et al. 2011b ApJ submitted <http://arxiv.org/abs/1108.1202>
- Blandford, R. D. & Rees, M. J., 1978, Proc. “Pittsburgh Conference on BL Lac objects”, 328
- Cutri, R. M. 2011, wise.rept, 1
- D’Abrusco, R., Massaro, F., Ajello, M., Grindlay, J. E., Smith, Howard A. & Tosti, G. 2012 ApJ accepted

---

<sup>7</sup><http://www.star.bris.ac.uk/~mbt/topcat/>

- Hartman, R.C. et al., 1999 ApJS 123
- Laurino, O. & D’Abrusco 2011 MNRAS in press
- Massaro, E., Giommi, P., Leto, C., Marchegiani, P., Maselli, A., Perri, M., Piranomonte, S., Sclavi, S. 2009 A&A, 495, 691
- Massaro, E., Giommi, P., Leto, C., Marchegiani, P., Maselli, A., Perri, M., Piranomonte, S., Sclavi, S. 2010 <http://arxiv.org/abs/1006.0922>
- Massaro, E., Giommi, P., Leto, C., Marchegiani, P., Maselli, A., Perri, M., Piranomonte, S., “Multifrequency Catalogue of Blazars (3rd Edition)”, ARACNE Editrice, Rome, Italy
- Massaro, F., D’Abrusco, R., Ajello, M., Grindlay, J. E. & Smith, H. A. 2011 ApJ, 740L, 48
- Massaro, F., D’Abrusco, R., Ajello, Gasparrini, d., Tosti, G., M., Grindlay, J. E. & Smith, H. A. 2012 ApJ submitted
- Massaro, F., D’Abrusco, R., Tosti, G. & Ajello, M. 2012b in preparation
- Taylor, M. B. 2005, ASP Conf. Ser., 347, 29
- Wright, E. L., et al. 2010 AJ, 140, 1868

Table 2: UGS Associations.

Name	distance (arcsec)	$c_{12}$	$\sigma_{12}$	$c_{23}$	$\sigma_{23}$	$c_{34}$	$\sigma_{34}$	$s_b$	$s_q$	class	$\pi$
2FGL J0038.8+6259											
J003818.70+630605.2	443.08	1.15	0.03	2.59	0.03	2.52	0.03	0.89	0.99	A	2/830
J003756.80+630459.2	492.33	0.67	0.04	2.09	0.06	2.36	0.12	0.40	0.00	B	3/830
J003834.17+630621.7	413.68	0.95	0.06	2.55	0.09	2.69	0.16	0.22	0.19	C	0/830
2FGL J0158.6+8558											
J014847.32+860345.3	707.33	1.21	0.03	3.10	0.03	2.66	0.05	0.29	0.73	A	1/2439
J015619.63+855634.6	173.64	1.11	0.04	3.49	0.04	2.71	0.05	0.00	0.70	B	0/2439
J014935.28+860115.3	603.41	0.73	0.03	2.34	0.05	2.06	0.16	0.44	0.21	B	0/2439
J015550.14+854745.1	644.48	1.15	0.04	2.51	0.06	2.20	0.19	0.26	0.37	B	0/2439
J015248.81+855703.5	376.98	1.11	0.05	2.96	0.08	1.87	0.29	0.21	0.22	C	0/2439
2FGL J0222.7+6820											
J022151.83+682414.0	375.72	0.45	0.03	2.0	0.04	2.17	0.07	0.61	0.00	B	0/642
2FGL J0226.1+0943											
J022634.26+093844.4	445.67	1.1	0.06	2.78	0.12	2.24	0.37	0.18	0.21	C	0/529
2FGL J0227.7+2249											
J022744.34+224834.3	73.27	0.98	0.04	2.53	0.05	1.91	0.13	0.47	0.26	B	0/621
2FGL J0237.9+5238											
J023749.24+523932.8	118.26	1.0	0.15	3.0	0.15	2.35	0.28	0.12	0.15	C	0/1330
2FGL J0251.0+2557											
J025144.37+255233.4	648.24	1.11	0.06	3.19	0.09	2.43	0.24	0.16	0.27	C	1/1587
2FGL J0307.4+4915											
J030727.22+491510.3	13.52	0.41	0.03	2.0	0.06	2.26	0.15	0.35	0.00	B	0/593
2FGL J0308.7+5954											
J030939.63+594254.9	838.69	1.1	0.04	2.67	0.06	2.18	0.14	0.39	0.39	A	0/4242
J030904.80+595515.7	163.43	0.72	0.04	2.04	0.06	2.08	0.11	0.46	0.00	B	0/4242
J030949.27+595443.4	497.05	1.27	0.04	3.45	0.05	2.54	0.07	0.00	0.56	B	0/4242
2FGL J0312.5−0914											
J031210.66−090902.3	494.53	1.1	0.06	2.84	0.12	2.85	0.25	0.12	0.2	C	2/898
J031152.05−092132.6	731.58	1.07	0.05	2.48	0.14	2.17	0.45	0.17	0.16	C	2/898
2FGL J0312.8+2013											
J031223.00+200749.5	505.2	1.01	0.05	2.43	0.14	2.29	0.4	0.19	0.15	C	1/512
2FGL J0318.0+0255											
J031820.31+025909.9	348.38	1.02	0.07	2.97	0.15	2.54	0.38	0.12	0.17	C	0/734
2FGL J0332.1+6309											
J033153.90+630814.1	114.51	0.98	0.04	2.4	0.05	1.85	0.15	0.39	0.18	B	0/1034
2FGL J0340.5+5307											
J034004.71+530127.6	476.7	1.13	0.05	2.75	0.07	2.34	0.17	0.34	0.34	B	0/2365
2FGL J0345.2−2356											
J034448.74−235653.1	373.57	1.18	0.07	3.16	0.11	2.24	0.37	0.11	0.19	C	0/622
2FGL J0404.0+3843											
J040520.96+384721.5	923.5	1.01	0.05	2.84	0.07	2.26	0.18	0.34	0.34	B	0/4315
2FGL J0404.6+5822											
J040400.59+582317.1	333.46	0.47	0.04	1.92	0.06	2.09	0.21	0.34	0.00	B	1/3481
J040628.51+582709.4	892.88	0.57	0.03	2.07	0.04	2.27	0.08	0.55	0.14	B	1/3481
2FGL J0409.8-0357											
J040946.57-040003.5	144.21	0.9	0.03	2.42	0.04	1.88	0.12	0.52	0.22	B	0/549
J041011.21-040000.0	319.59	0.99	0.06	2.91	0.13	2.31	0.37	0.14	0.19	C	1/549
2FGL J0414.9-0855											
J041457.01-085651.9	99.2	0.99	0.04	2.66	0.08	2.39	0.21	0.31	0.32	B	0/1182

Table 3: UGS Associations.

Name	distance (arcsec)	$c_{12}$	$\sigma_{12}$	$c_{23}$	$\sigma_{23}$	$c_{34}$	$\sigma_{34}$	$s_b$	$s_q$	class	$\pi$
2FGL J0416.0–4355											
J041605.81–435514.6	47.18	1.13	0.04	2.94	0.04	2.37	0.08	0.58	0.58	A	0/2603
J041442.89–434935.4	943.62	1.03	0.04	2.9	0.07	2.43	0.2	0.32	0.34	B	2/2603
J041506.36–440958.9	1045.16	1.08	0.04	2.74	0.06	2.14	0.18	0.36	0.38	B	2/2603
J041538.31–440412.8	568.43	1.01	0.05	2.6	0.1	2.49	0.3	0.21	0.23	C	1/2603
J041709.78–435922.4	751.76	1.04	0.08	2.94	0.16	2.5	0.45	0.11	0.15	C	1/2603
2FGL J0420.9–3743											
J042025.09–374444.5	368.83	0.82	0.04	2.5	0.09	2.41	0.28	0.25	0.17	B	1/1249
2FGL J0428.0–3845											
J042721.64–390100.6	1039.57	1.09	0.04	2.76	0.05	2.62	0.11	0.42	0.48	A	0/2563
2FGL J0458.4+0654											
J045911.96+065932.7	775.68	1.14	0.06	3.02	0.12	2.6	0.28	0.16	0.23	C	0/1476
2FGL J0515.0–4411											
J051322.89–441947.8	1153.62	1.01	0.04	3.02	0.05	2.38	0.13	0.35	0.46	A	1/3932
J051439.26–441348.7	258.38	1.11	0.06	3.28	0.09	2.48	0.21	0.16	0.28	C	3/3932
J051524.23–441457.2	308.78	1.15	0.06	2.85	0.11	2.28	0.38	0.14	0.22	C	3/3932
J051525.83–435632.7	962.23	1.02	0.06	2.96	0.1	2.23	0.32	0.21	0.22	C	3/3932
J051432.40–435214.3	1221.78	1.16	0.06	3.09	0.12	2.74	0.29	0.11	0.21	C	3/3932
2FGL J0529.3+3821											
J053006.26+382649.0	604.83	0.98	0.03	2.92	0.03	2.74	0.04	0.56	0.7	A	0/1574
J052939.38+382327.1	230.39	1.02	0.05	2.67	0.1	2.45	0.17	0.3	0.31	B	0/1574
J052943.26+382049.3	231.47	1.1	0.05	2.84	0.07	2.14	0.19	0.31	0.34	B	0/1574
J052941.52+382442.2	298.7	0.69	0.03	2.43	0.05	2.18	0.1	0.53	0.25	B	0/1574
J053006.35+382532.8	566.64	0.89	0.05	2.29	0.09	2.2	0.28	0.27	0.15	B	0/1574
J053018.78+382231.9	653.47	1.01	0.05	2.62	0.07	2.37	0.21	0.3	0.29	B	0/1574
2FGL J0540.1–7554											
J054003.36–754157.9	736.81	1.06	0.04	2.76	0.04	2.49	0.1	0.51	0.52	A	0/3412
J054231.99–760139.4	677.11	1.0	0.04	2.84	0.08	2.42	0.23	0.29	0.31	B	1/3412
J053926.22–760648.6	772.37	0.91	0.05	2.71	0.08	2.64	0.21	0.24	0.24	B	1/3412
J054111.58–760247.1	557.16	1.06	0.05	2.82	0.08	2.81	0.2	0.18	0.26	C	0/3412
2FGL J0545.6+6018											
J054610.69+602331.6	368.05	1.11	0.05	2.85	0.07	2.5	0.16	0.32	0.35	B	0/449
2FGL J0555.9–4348											
J055601.91–433947.3	513.92	1.07	0.04	2.55	0.06	2.35	0.18	0.38	0.38	A	0/2668
J055618.73–435146.1	338.08	0.93	0.04	2.51	0.05	2.13	0.14	0.46	0.33	B	0/2668
J055432.27–435241.2	927.17	0.89	0.04	2.68	0.07	2.12	0.26	0.32	0.21	B	0/2668
J055531.86–435706.1	584.44	0.94	0.05	2.9	0.1	2.32	0.3	0.18	0.23	C	2/2668
2FGL J0600.8–1949											
J060120.34–200725.5	1130.75	1.03	0.03	2.64	0.04	2.09	0.08	0.62	0.63	A	0/4104
J055931.95–195135.0	1131.41	1.13	0.06	3.1	0.1	2.22	0.35	0.16	0.21	C	1/4104
2FGL J0600.9+3839											
J060102.86+383829.6	68.68	0.97	0.04	2.54	0.08	2.38	0.19	0.33	0.28	B	0/613
2FGL J0602.7–4011											
J060237.09–401453.5	239.84	0.97	0.03	2.48	0.04	2.3	0.07	0.63	0.51	A	0/1127
J060251.28–401845.1	472.64	0.88	0.04	2.44	0.04	1.82	0.11	0.53	0.22	B	0/1127
J060254.77–402035.2	588.88	1.12	0.06	2.95	0.12	2.49	0.32	0.18	0.22	C	2/1127



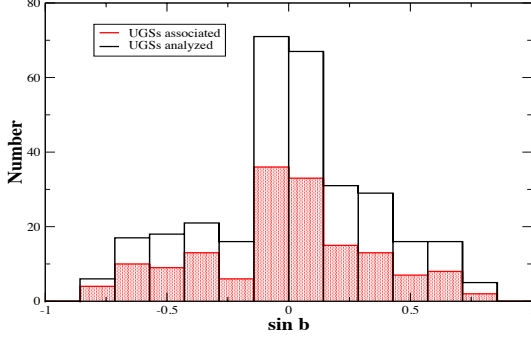


Fig. 3.— The distribution of the Galactic latitude for all the UGSs analyzed in comparison with that for the 156 associated by our procedure.

Table 4: UGS Associations.

Name	distance (arcsec)	$c_{12}$	$\sigma_{12}$	$c_{23}$	$\sigma_{23}$	$c_{34}$	$\sigma_{34}$	$s_b$	$s_q$	class	$\pi$
2FGL J0608.3+2037											
J060835.36+203604.1	237.43	1.03	0.03	2.83	0.03	2.22	0.05	0.76	0.77	A	0/1130
J060831.76+203141.8	405.85	1.03	0.03	2.47	0.03	2.32	0.03	0.91	0.88	A	0/1130
J060740.08+203959.2	579.55	1.11	0.04	2.86	0.04	2.37	0.09	0.57	0.58	A	0/1130
J060803.38+204111.0	309.04	1.24	0.03	2.55	0.03	2.56	0.03	0.00	0.7	B	2/1130
J060831.63+204122.5	260.5	1.19	0.04	2.82	0.09	2.74	0.12	0.18	0.32	C	0/1130
2FGL J0616.6+2425											
J061623.95+241809.2	458.21	0.98	0.03	3.38	0.04	2.8	0.04	0.00	0.56	B	1/5456
J061609.79+241911.1	513.16	0.66	0.03	2.37	0.03	1.72	0.08	0.63	0.21	B	1/5456
J061705.49+240850.4	1063.29	0.53	0.04	2.17	0.07	1.87	0.24	0.34	0.00	B	1/5456
J061611.60+241917.2	491.67	0.94	0.04	2.15	0.06	2.8	0.12	0.23	0.2	C	1/5456
J061600.61+242253.6	506.98	0.84	0.06	2.78	0.11	2.44	0.28	0.17	0.14	C	1/5456
J061640.77+241151.1	806.78	0.98	0.06	2.78	0.09	1.84	0.41	0.18	0.16	C	1/5456
J061650.09+244221.1	1042.8	1.2	0.08	3.03	0.1	2.44	0.24	0.11	0.23	C	1/5456
2FGL J0620.8–2556											
J062108.67–255758.1	222.84	0.96	0.05	2.7	0.09	2.08	0.35	0.23	0.21	C	1/3508
2FGL J0631.7+0428											
J063151.53+041903.3	581.96	0.93	0.03	2.76	0.03	2.46	0.06	0.69	0.67	A	1/9083
J063155.40+041844.1	612.84	1.09	0.04	2.95	0.09	2.72	0.12	0.27	0.38	A	1/9083
J063103.52+042739.6	624.47	0.71	0.04	2.36	0.07	1.88	0.38	0.28	0.14	B	1/9083
J063239.59+043629.4	941.7	0.81	0.04	2.53	0.09	1.71	0.32	0.26	0.14	B	1/9083
J063048.95+043714.4	986.14	0.7	0.03	1.99	0.09	2.02	0.3	0.3	0.00	B	1/9083
J063147.96+045049.0	1332.46	0.62	0.04	2.26	0.08	2.35	0.14	0.35	0.00	B	1/9083
J063314.27+042905.5	1333.84	0.6	0.03	2.1	0.12	1.83	0.31	0.26	0.07	B	1/9083
2FGL J0644.6+6034											
J064459.38+603132.1	223.54	1.01	0.04	2.69	0.06	2.52	0.15	0.38	0.4	A	0/877
J064417.82+603932.2	347.48	1.2	0.06	3.19	0.1	2.74	0.22	0.1	0.26	C	0/877
2FGL J0647.7+0032											
J064712.98+003702.8	545.46	1.12	0.04	3.07	0.05	2.19	0.08	0.51	0.51	A	0/2093
J064718.24+003250.6	384.38	0.81	0.04	2.59	0.11	2.31	0.2	0.29	0.21	B	0/2093
2FGL J0713.5–0952											
J071337.47–101207.9	1182.86	0.98	0.04	2.82	0.05	2.23	0.1	0.49	0.49	A	1/11990
J071400.29–095518.9	429.54	1.14	0.07	2.93	0.08	2.72	0.14	0.19	0.31	C	2/11990
2FGL J0723.9+2901											
J072354.83+285929.9	153.39	1.15	0.05	2.93	0.05	2.3	0.12	0.38	0.43	A	0/1215
2FGL J0725.8–0549											
J072536.62–055807.3	558.18	1.06	0.04	2.74	0.04	2.14	0.09	0.55	0.56	A	0/1094
2FGL J0737.1–3235											
J073738.91–323256.6	385.01	1.13	0.06	3.27	0.05	2.55	0.08	0.22	0.49	B	1/1985
J073646.70–324215.2	516.85	0.63	0.04	2.28	0.07	1.72	0.31	0.27	0.1	B	1/1985
2FGL J0737.5–8246											
J073713.75–824812.8	111.61	1.02	0.06	3.08	0.11	2.24	0.36	0.16	0.2	C	0/916
J073715.07–825511.4	525.59	0.89	0.05	2.89	0.07	2.0	0.23	0.23	0.24	C	0/916

Table 5: UGS Associations.

Name	distance (arcsec)	$c_{12}$	$\sigma_{12}$	$c_{23}$	$\sigma_{23}$	$c_{34}$	$\sigma_{34}$	$s_b$	$s_q$	class	$\pi$
2FGL J0742.7–3113											
J074226.42–305720.1	990.78	1.09	0.03	2.73	0.03	2.22	0.03	0.9	0.91	A	1/3499
J074345.64–310758.0	873.05	1.02	0.05	2.29	0.05	2.16	0.15	0.31	0.25	B	1/3499
J074303.55–312057.4	522.58	1.2	0.1	2.78	0.08	2.0	0.29	0.1	0.18	C	2/3499
2FGL J0744.1–2523											
J074406.14–252154.1	142.98	1.27	0.03	2.55	0.03	1.98	0.05	0.00	0.44	B	0/630
J074401.10–252203.9	180.53	1.26	0.06	2.77	0.04	2.66	0.08	0.00	0.5	B	0/630
J074359.96–252220.6	183.53	0.93	0.05	2.86	0.06	2.53	0.18	0.27	0.33	B	0/630
J074356.53–251909.8	351.78	1.1	0.09	2.87	0.1	2.69	0.21	0.14	0.22	C	0/630
2FGL J0745.5+7910											
J074502.17+791110.5	98.65	1.04	0.07	2.83	0.14	2.39	0.43	0.16	0.18	C	0/1343
J074659.63+790356.7	469.93	1.14	0.05	2.67	0.1	2.72	0.23	0.17	0.24	C	0/1343
2FGL J0746.0–0222											
J074627.02–022549.4	391.79	0.65	0.04	2.08	0.07	2.18	0.27	0.29	0.00	B	1/1597
J074534.78–021534.7	604.93	1.13	0.04	2.9	0.06	2.42	0.18	0.34	0.36	B	1/1597
2FGL J0748.5–2204											
J074726.63–220630.9	935.48	1.0	0.04	2.89	0.03	2.29	0.07	0.65	0.66	A	0/4863
2FGL J0753.2+1937											
J075217.84+193542.3	839.58	1.16	0.03	2.97	0.03	2.65	0.03	0.53	0.93	A	0/1565
2FGL J0753.2–1634											
J075313.37–160833.2	1560.13	1.29	0.05	2.99	0.06	2.59	0.13	0.00	0.39	B	6/15814
J075249.51–160820.5	1618.57	0.92	0.04	2.95	0.05	2.64	0.09	0.23	0.45	B	6/15814
J075213.04–160415.1	2032.41	1.11	0.06	2.75	0.11	2.86	0.25	0.13	0.2	C	0/15814
2FGL J0900.9+6736											
J090121.65+673955.5	228.51	0.9	0.05	2.67	0.11	2.34	0.31	0.23	0.21	C	2/1220
2FGL J1032.9–8401											
J103015.41–840308.2	274.15	0.95	0.04	2.6	0.05	2.04	0.16	0.41	0.32	B	0/1438
2FGL J1058.7–6621											
J105854.76–663412.8	736.6	0.93	0.07	2.62	0.07	2.54	0.17	0.27	0.25	B	1/1609
2FGL J1104.7–6036											
J110500.45–603559.0	117.21	0.76	0.08	2.04	0.08	1.85	0.22	0.25	0.11	B	0/235
2FGL J1105.4–7622											
J110409.06–762719.3	413.02	0.78	0.02	2.59	0.02	2.07	0.03	1.21	0.73	A	0/1918
J110632.74–762521.1	293.54	0.56	0.03	1.79	0.06	1.97	0.22	0.38	0.00	B	1/1918
J110746.55–761517.6	644.16	0.65	0.03	1.75	0.04	2.25	0.07	0.46	0.00	B	1/1918
2FGL J1105.6–6114											
J110641.59–611126.7	486.49	1.13	0.1	2.9	0.14	2.69	0.25	0.11	0.18	C	0/1650
J110709.52–611247.7	664.92	1.15	0.06	2.87	0.14	2.51	0.2	0.19	0.25	C	0/1650
2FGL J1207.3–5055											
J120715.61–504558.3	595.37	0.99	0.04	2.98	0.04	2.19	0.1	0.4	0.51	A	0/2542
J120750.50–510314.6	523.02	1.12	0.07	2.8	0.12	2.72	0.25	0.15	0.18	C	2/2542
2FGL J1214.1–4410											
J121305.50–440807.3	667.39	0.85	0.03	2.63	0.03	2.46	0.04	0.82	0.66	A	0/1816
J121442.80–441338.0	445.13	1.09	0.05	2.88	0.09	2.84	0.2	0.17	0.25	C	0/1816
2FGL J1236.1–6155											
J123550.23–614507.5	629.83	0.93	0.04	2.43	0.05	2.41	0.1	0.48	0.34	B	0/1868
J123452.66–614702.4	739.59	0.9	0.04	2.29	0.03	2.1	0.03	0.87	0.36	B	0/1868
J123500.79–615611.1	489.18	0.96	0.06	2.98	0.09	2.12	0.21	0.21	0.25	C	1/1868
J123551.88–614523.2	611.92	1.18	0.04	2.55	0.09	2.07	0.22	0.16	0.28	C	1/1868

Table 6: UGS Associations.

Name	distance (arcsec)	$c_{12}$	$\sigma_{12}$	$c_{23}$	$\sigma_{23}$	$c_{34}$	$\sigma_{34}$	$s_b$	$s_g$	class	$\pi$
2FGL J1243.9–6232											
J124252.40–623214.0	437.79	1.13	0.04	2.52	0.04	2.52	0.04	0.63	0.64	A	0/854
J124322.29–623912.7	466.0	0.7	0.08	2.41	0.07	2.29	0.15	0.3	0.09	B	0/854
J124438.34–623425.2	317.58	0.85	0.06	2.3	0.11	2.6	0.15	0.24	0.14	C	0/854
2FGL J1248.6–5510											
J124946.06–550758.3	602.9	1.03	0.05	2.7	0.07	2.45	0.15	0.36	0.36	B	2/4244
2FGL J1255.8–5828											
J125459.46–582009.4	636.52	1.32	0.05	2.82	0.04	2.19	0.06	0.00	0.53	B	0/12152
J125357.08–583322.2	945.84	0.65	0.04	2.22	0.03	1.49	0.03	0.9	0.34	B	0/12152
J125448.95–585010.1	1399.83	1.06	0.1	2.84	0.06	2.34	0.11	0.33	0.33	B	0/12152
J125646.35–581306.0	1009.28	1.13	0.11	2.45	0.09	2.48	0.2	0.12	0.17	C	2/12152
2FGL J1317.2–6304											
J131818.06–630215.1	456.0	0.87	0.09	2.85	0.1	2.03	0.24	0.16	0.14	C	0/1382
2FGL J1320.1–5756											
J131938.49–575738.1	271.56	1.13	0.12	2.45	0.11	2.36	0.25	0.1	0.16	C	0/1294
2FGL J1324.4–5411											
J132530.49–542548.7	999.54	1.13	0.09	2.77	0.09	2.34	0.26	0.18	0.22	C	0/3899
2FGL J1339.2–2348											
J133901.75–240113.9	762.96	1.09	0.04	2.94	0.04	2.26	0.07	0.61	0.61	A	0/1337
J133825.70–235150.2	678.03	1.09	0.04	3.19	0.06	2.98	0.09	0.00	0.38	B	0/1337
2FGL J1345.8–3356											
J134543.05–335643.3	94.27	0.85	0.04	2.35	0.08	2.02	0.3	0.28	0.13	B	0/2098
J134515.46–334917.7	612.18	0.91	0.06	2.81	0.14	2.56	0.34	0.13	0.16	C	1/2098
2FGL J1347.0–2956											
J134706.88–295842.4	134.22	0.78	0.04	2.19	0.1	2.05	0.32	0.26	0.11	B	0/729
J134742.26–300046.8	576.17	1.19	0.05	3.07	0.07	2.44	0.18	0.17	0.33	C	0/729
2FGL J1407.4–2948											
J140657.64–301718.0	1737.44	1.15	0.07	2.69	0.15	2.45	0.43	0.12	0.17	C	4/7776
2FGL J1414.1–5450											
J141236.97–543952.4	1009.62	0.99	0.04	2.32	0.05	2.32	0.1	0.46	0.35	B	1/4045
J141349.58–544243.4	475.18	0.99	0.1	2.93	0.11	2.53	0.23	0.15	0.21	C	1/4045
J141337.01–550126.7	736.43	0.93	0.08	2.4	0.11	2.42	0.21	0.22	0.16	C	1/4045
2FGL J1417.5–4404											
J141721.43–435342.9	668.44	1.02	0.07	2.88	0.09	2.48	0.22	0.23	0.26	C	1/2016
2FGL J1422.3–6841											
J142409.23–683715.6	660.57	0.68	0.04	2.1	0.04	1.83	0.1	0.53	0.22	B	0/1482
2FGL J1423.9–7842											
J142343.58–782934.3	801.85	1.04	0.06	2.82	0.12	2.91	0.24	0.11	0.19	C	2/2721

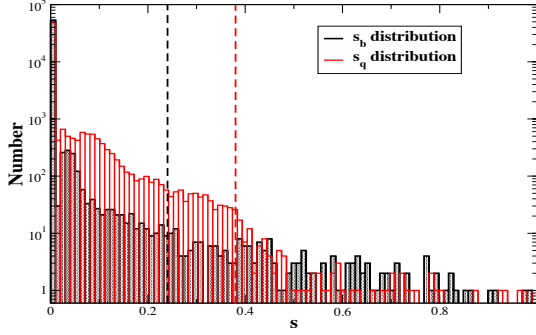


Fig. 4.— The distribution of the  $s_b$  (black) and  $s_q$  (red) parameters for all the 55195 *WISE* source within all the ROCs defined for the 313 UGSs analyzed. The vertical lines corresponds to the thresholds for the  $s_b$  and  $s_q$  parameters to determine the blazar classes (see Section 3.2).

Table 7: UGS Associations.

Name	distance (arcsec)	$c_{12}$	$\sigma_{12}$	$c_{23}$	$\sigma_{23}$	$c_{34}$	$\sigma_{34}$	$s_b$	$s_q$	class	$\pi$
2FGL J1517.2+3645											
J151649.27+365022.9	420.93	1.05	0.05	2.63	0.09	2.48	0.24	0.27	0.27	B	0/1352
J151752.13+364125.5	508.82	1.04	0.04	3.01	0.06	2.19	0.19	0.34	0.36	B	0/1352
2FGL J1518.4–5233											
J151807.33–523431.0	184.75	0.66	0.07	2.31	0.05	1.41	0.17	0.26	0.13	B	0/979
2FGL J1543.7–0241											
J154315.19–022531.4	1052.36	1.06	0.08	2.85	0.18	2.58	0.43	0.11	0.14	C	0/3462
2FGL J1552.8–4824											
J155237.30–484152.9	1044.56	0.98	0.05	2.7	0.04	2.45	0.06	0.54	0.53	A	0/5499
2FGL J1553.5–0324											
J155341.52–031231.4	698.12	1.35	0.04	2.68	0.05	2.37	0.11	0.00	0.42	B	0/2108
J155314.95–031204.8	778.98	0.95	0.05	2.59	0.09	2.21	0.24	0.27	0.24	B	0/2108
J155306.36–032317.7	432.95	0.92	0.05	2.36	0.11	2.5	0.28	0.24	0.16	C	1/2108
2FGL J1612.0+1403											
J161148.58+135716.8	426.68	1.07	0.05	3.09	0.09	2.16	0.33	0.16	0.22	C	0/2763
J161118.10+140328.9	616.83	1.12	0.06	3.14	0.09	2.59	0.21	0.17	0.28	C	0/2763
2FGL J1614.8+4703											
J161434.68+470420.3	178.15	1.09	0.03	3.15	0.03	2.1	0.04	0.51	0.82	A	0/3922
J161541.22+471111.8	701.47	0.75	0.04	2.27	0.05	2.26	0.13	0.48	0.23	B	3/3922
J161450.96+465954.1	200.29	1.18	0.05	2.8	0.09	2.45	0.24	0.21	0.28	C	1/3922
J161513.04+471356.0	680.29	1.06	0.06	2.95	0.13	2.34	0.42	0.17	0.19	C	1/3922
J161536.97+471711.1	959.75	1.24	0.06	2.83	0.11	2.28	0.36	0.1	0.21	C	1/3922
2FGL J1617.6–4219											
J161955.00–422815.1	1557.87	1.05	0.05	2.85	0.04	2.58	0.06	0.52	0.58	A	0/7942
J161804.21–421209.0	524.8	0.97	0.05	2.22	0.05	2.23	0.09	0.38	0.27	B	0/7942
2FGL J1619.0–4650											
J161922.19–464331.6	472.97	0.66	0.04	2.14	0.04	1.88	0.05	0.69	0.29	B	5/17602
J161926.88–463511.1	964.94	1.01	0.04	2.48	0.04	1.92	0.07	0.62	0.35	B	5/17602
J161929.08–463501.3	980.05	0.54	0.04	2.35	0.05	2.02	0.09	0.32	0.00	B	5/17602
2FGL J1619.6–4509											
J161944.64–451147.4	145.23	0.6	0.07	2.24	0.06	2.25	0.12	0.35	0.07	B	1/2541
2FGL J1622.8–0314											
J162225.36–031439.0	414.55	1.18	0.06	3.18	0.1	2.66	0.2	0.11	0.27	C	0/1577

Table 8: UGS Associations.

Name	distance (arcsec)	$c_{12}$	$\sigma_{12}$	$c_{23}$	$\sigma_{23}$	$c_{34}$	$\sigma_{34}$	$s_b$	$s_q$	class	$\pi$
2FGL J1623.2+4328											
J162324.12+432533.8	183.07	0.91	0.04	2.64	0.06	2.47	0.14	0.41	0.35	B	0/1983
J162237.62+433801.8	720.08	1.13	0.05	2.92	0.08	2.25	0.24	0.29	0.3	B	0/1983
2FGL J1624.2–2124											
J162608.57–211709.1	1617.78	1.38	0.04	2.79	0.06	2.57	0.12	0.00	0.4	B	0/17861
2FGL J1627.8+3219											
J162800.41+322414.9	319.07	1.12	0.05	2.89	0.09	2.52	0.27	0.21	0.26	C	1/1045
2FGL J1630.2–4752											
J162957.80–475327.5	189.16	0.73	0.05	1.88	0.05	1.44	0.22	0.25	0.15	B	0/539
2FGL J1631.0–1050											
J163204.19–104411.5	1008.36	0.89	0.04	2.56	0.06	1.89	0.19	0.38	0.18	B	0/3687
2FGL J1641.8–5319											
J164059.69–532258.6	509.89	0.97	0.19	2.57	0.11	2.55	0.15	0.17	0.15	C	0/2000
2FGL J1643.3–4928											
J164153.54–491752.0	1067.61	0.7	0.03	2.29	0.03	2.1	0.02	1.01	0.42	A	1/3888
2FGL J1647.0+4351											
J164652.47+435821.7	434.78	0.97	0.04	2.86	0.07	2.58	0.16	0.31	0.36	B	0/2415
J164720.15+434438.6	441.88	0.86	0.05	2.69	0.09	2.54	0.23	0.27	0.2	B	0/2415
J164808.75+435530.4	734.82	0.86	0.05	2.73	0.1	2.23	0.34	0.19	0.17	C	3/2415
2FGL J1653.6–0159											
J165315.62–015822.3	324.68	1.02	0.04	2.37	0.04	1.84	0.12	0.45	0.25	B	0/335
2FGL J1656.4–0738											
J165639.14–073821.1	142.99	1.21	0.04	2.85	0.05	2.36	0.11	0.22	0.45	B	0/1591
2FGL J1657.5–4652											
J165708.90–464752.2	377.56	0.82	0.02	2.09	0.03	1.58	0.03	1.13	0.47	A	0/1009
J165744.80–464635.7	370.78	0.59	0.05	1.72	0.09	1.91	0.18	0.26	0.00	B	0/1009
2FGL J1704.3+1235											
J170409.58+123422.0	170.99	0.74	0.04	2.12	0.07	1.57	0.41	0.24	0.12	B	0/1044
J170418.39+123057.4	293.74	1.13	0.04	2.71	0.08	2.18	0.26	0.26	0.29	B	0/1044
2FGL J1704.9–4618											
J170503.47–462929.4	676.28	1.12	0.04	2.59	0.03	2.37	0.04	0.75	0.76	A	0/6392
J170511.74–462809.5	608.53	0.57	0.03	2.2	0.03	2.03	0.03	0.91	0.00	B	5/6392
J170410.40–462600.8	689.62	0.43	0.04	2.16	0.03	2.15	0.03	0.51	0.00	B	5/6392
J170556.65–462409.7	690.38	0.53	0.03	1.74	0.03	1.97	0.05	0.71	0.00	B	5/6392
2FGL J1710.0–0323											
J170853.49–032323.4	1078.67	0.96	0.05	2.56	0.11	2.59	0.25	0.22	0.19	C	0/6212
J170911.00–033720.7	1160.96	1.01	0.07	2.77	0.16	2.81	0.31	0.11	0.15	C	0/6212
J171053.82–030442.3	1344.04	1.12	0.06	2.87	0.09	2.78	0.16	0.18	0.29	C	0/6212
2FGL J1710.5–5020											
J171141.00–502817.2	803.32	0.98	0.06	2.56	0.05	1.98	0.11	0.41	0.3	B	0/2260

Table 9: UGS Associations.

Name	distance (arcsec)	$c_{12}$	$\sigma_{12}$	$c_{23}$	$\sigma_{23}$	$c_{34}$	$\sigma_{34}$	$s_b$	$s_q$	class	$\pi$
2FGL J1726.6–3545											
J172706.54–354400.0	332.55	0.83	0.05	2.26	0.05	1.95	0.16	0.38	0.16	B	6/2747
J172645.15–355126.8	340.31	0.78	0.04	1.97	0.04	2.01	0.06	0.52	0.00	B	6/2747
J172743.40–355104.9	823.97	0.75	0.05	1.97	0.06	1.8	0.14	0.38	0.16	B	6/2747
2FGL J1727.6+0647											
J172644.95+063918.6	964.35	1.1	0.05	2.91	0.08	2.46	0.21	0.28	0.3	B	0/3011
J172743.08+063729.0	610.69	0.88	0.06	2.79	0.13	2.16	0.41	0.15	0.16	C	0/3011
2FGL J1729.5–0854											
J172917.32–085503.3	214.0	1.3	0.04	2.73	0.06	2.63	0.11	0.00	0.43	B	1/4158
2FGL J1730.6–0353											
J173052.85–035247.1	223.9	1.27	0.04	2.94	0.04	2.13	0.1	0.00	0.49	B	0/1447
2FGL J1730.8+5427											
J173238.56+543233.4	952.59	1.09	0.04	2.66	0.05	2.53	0.14	0.44	0.42	A	0/5245
J173145.57+540836.1	1246.33	1.12	0.05	2.74	0.09	2.27	0.32	0.24	0.26	B	3/5245
J173018.81+543700.6	622.98	1.07	0.07	2.97	0.17	2.43	0.49	0.1	0.15	C	6/5245
J172953.81+541836.0	768.47	1.06	0.06	2.8	0.11	2.58	0.3	0.18	0.22	C	6/5245
J173014.69+540822.6	1223.9	1.0	0.06	2.9	0.12	2.1	0.44	0.17	0.17	C	6/5245
2FGL J1734.7–2533											
J173414.24–253645.5	456.0	0.73	0.03	2.21	0.03	1.42	0.03	0.81	0.38	B	3/2555
2FGL J1739.6–2726											
J173943.37–272858.7	181.4	0.52	0.05	2.11	0.03	1.61	0.03	0.72	0.00	B	11/4288
2FGL J1741.1–6750											
J174046.15–674325.0	471.78	1.15	0.05	2.86	0.07	2.24	0.2	0.29	0.34	B	0/2877
J174059.77–680132.3	634.08	1.06	0.06	2.46	0.1	2.55	0.26	0.18	0.21	C	2/2877

Table 10: UGS Associations.

Name	distance (arcsec)	$c_{12}$	$\sigma_{12}$	$c_{23}$	$\sigma_{23}$	$c_{34}$	$\sigma_{34}$	$s_b$	$s_q$	class	$\pi$
2FGL J1742.5–3323											
J174220.74–333005.4	414.44	0.55	0.11	2.26	0.08	2.14	0.06	0.28	0.07	B	13/2475
2FGL J1743.2–2304											
J174224.66–225942.4	710.92	1.02	0.06	2.56	0.04	1.88	0.04	0.58	0.35	B	0/3656
2FGL J1745.6+0203											
J174526.95+020532.7	208.91	1.06	0.04	2.63	0.04	2.19	0.08	0.57	0.57	A	0/4745
J174647.05+020925.9	1066.59	1.07	0.04	2.61	0.06	2.27	0.16	0.38	0.39	A	0/4745
J174507.82+015442.5	729.02	1.32	0.03	3.5	0.03	2.4	0.03	0.00	0.7	B	0/4745
2FGL J1746.5–3238											
J174609.56–323717.1	326.79	0.79	0.04	2.11	0.03	1.59	0.03	0.82	0.35	B	1/436
2FGL J1747.2–3507											
J174753.04–352154.3	975.52	0.75	0.03	2.35	0.03	1.78	0.02	1.01	0.43	A	0/3389
J174741.23–350334.3	385.87	0.72	0.04	1.97	0.03	1.34	0.03	0.87	0.36	B	6/3389
2FGL J1748.6–2913											
J174832.69–291040.8	210.12	0.48	0.05	1.74	0.06	2.09	0.09	0.36	0.00	B	0/518
J174830.54–291822.6	292.64	0.68	0.04	2.0	0.03	1.49	0.05	0.67	0.28	B	0/518
J174838.23–291609.7	137.48	1.16	0.2	2.78	0.11	2.77	0.1	0.1	0.17	C	0/518
2FGL J1749.1+0515											
J174850.00+050822.5	540.35	1.23	0.06	3.1	0.08	2.86	0.15	0.11	0.3	C	0/2912
2FGL J1754.1–2930											
J175438.09–291752.5	850.88	0.65	0.04	2.11	0.03	1.4	0.02	0.84	0.39	A	0/3242
J175414.40–293326.6	187.81	0.83	0.12	2.08	0.07	1.34	0.06	0.26	0.15	B	9/3242
J175304.57–292725.2	860.74	0.69	0.15	2.09	0.09	1.72	0.06	0.3	0.11	B	9/3242
2FGL J1759.2–3853											
J175903.29–384739.5	401.59	0.61	0.04	2.03	0.03	1.44	0.03	0.82	0.38	A	0/1855

Table 11: UGS Associations.

Name	distance (arcsec)	$c_{12}$	$\sigma_{12}$	$c_{23}$	$\sigma_{23}$	$c_{34}$	$\sigma_{34}$	$s_b$	$s_q$	class	$\pi$
2FGL J1802.8–6706											
J180100.62–670503.7	647.12	1.0	0.04	3.12	0.06	2.47	0.13	0.00	0.41	B	1/3111
2FGL J1811.3–2421											
J181126.39–240459.9	1018.47	0.84	0.04	2.74	0.03	2.56	0.03	0.65	0.56	A	0/4178
2FGL J1813.6–2821											
J181345.24–283058.6	594.38	0.75	0.04	2.26	0.03	2.1	0.02	0.94	0.4	A	0/1731
2FGL J1819.3–1523											
J181947.65–152807.1	479.71	0.66	0.11	2.22	0.11	2.12	0.12	0.25	0.1	B	1/1363
2FGL J1821.8+0830											
J182134.70+084319.1	802.9	1.15	0.09	2.87	0.13	2.6	0.28	0.14	0.18	C	0/2585
2FGL J1824.5+1013											
J182448.39+100712.6	423.77	1.19	0.06	2.76	0.06	2.1	0.17	0.27	0.35	B	0/1066
2FGL J1827.6+1149											
J182721.63+114844.0	265.97	1.11	0.07	2.57	0.11	2.43	0.3	0.17	0.2	C	0/2202
2FGL J1831.2–1518											
J183033.83–151412.0	651.32	0.89	0.04	2.59	0.05	1.76	0.12	0.42	0.18	B	2/4390
J183205.20–152327.9	782.97	0.85	0.07	2.23	0.06	1.54	0.12	0.31	0.15	B	2/4390
J183050.58–153533.2	1104.95	0.46	0.04	1.85	0.03	1.71	0.03	0.74	0.23	B	2/4390
2FGL J1832.0–0200											
J183208.77–015414.2	421.64	0.72	0.04	2.18	0.05	2.04	0.12	0.44	0.18	B	0/1036
2FGL J1832.2–6502											
J183256.27–651006.5	535.98	1.17	0.06	2.91	0.12	2.77	0.26	0.12	0.22	C	0/1700
2FGL J1835.4+1036											
J183551.92+103056.8	510.44	1.04	0.04	2.94	0.04	2.55	0.07	0.52	0.61	A	0/2844

Table 12: UGS Associations.

Name	distance (arcsec)	$c_{12}$	$\sigma_{12}$	$c_{23}$	$\sigma_{23}$	$c_{34}$	$\sigma_{34}$	$s_b$	$s_g$	<i>class</i>	$\pi$
2FGL J1835.4+1349											
J183522.00+135733.9	484.14	1.15	0.06	2.78	0.06	2.28	0.13	0.33	0.38	A	1/2344
J183535.35+134848.9	141.16	0.78	0.04	2.26	0.05	2.02	0.15	0.44	0.19	B	1/2344
J183539.22+135055.0	206.92	1.22	0.04	2.82	0.06	2.67	0.11	0.19	0.44	B	1/2344
2FGL J1835.5–0649											
J183538.53–064854.2	71.66	0.61	0.04	1.74	0.04	2.12	0.09	0.55	0.00	B	0/622
J183554.30–065518.0	427.7	0.74	0.05	1.88	0.05	1.96	0.09	0.39	0.00	B	0/622
2FGL J1837.9+3821											
J183656.31+382233.2	692.72	1.21	0.04	2.92	0.05	2.51	0.1	0.22	0.5	B	0/6850
J183816.58+383708.9	992.13	1.33	0.03	2.93	0.04	2.52	0.08	0.00	0.59	B	0/6850
J183812.98+380159.9	1170.32	0.99	0.05	2.42	0.09	2.33	0.28	0.27	0.21	B	0/6850
J183753.23+384500.2	1429.91	1.34	0.04	2.98	0.04	2.2	0.08	0.00	0.55	B	0/6850
J183742.09+381955.6	167.03	1.14	0.06	2.75	0.1	2.16	0.36	0.18	0.23	C	2/6850
J183828.81+382705.1	534.57	0.99	0.05	2.45	0.12	2.6	0.3	0.2	0.17	C	2/6850
J183836.32+382924.4	694.43	1.22	0.06	3.06	0.1	2.67	0.26	0.11	0.25	C	2/6850
J183746.20+380846.5	750.76	1.04	0.07	2.85	0.13	2.69	0.3	0.14	0.18	C	2/6850
J183642.07+381203.1	1016.29	1.05	0.07	3.06	0.13	2.17	0.47	0.12	0.16	C	2/6850
2FGL J1839.0–0102											
J183839.61–010614.0	435.0	0.85	0.04	2.69	0.03	2.21	0.04	0.79	0.48	A	1/1441
2FGL J1842.3–5839											
J184317.58–583752.0	452.64	1.25	0.05	2.91	0.07	2.72	0.13	0.00	0.38	B	1/883
J184240.89–584439.7	340.91	0.95	0.07	2.99	0.11	2.91	0.21	0.11	0.16	C	0/883
2FGL J1844.3+1548											
J184425.36+154645.9	150.64	0.91	0.03	2.36	0.04	1.95	0.09	0.57	0.24	B	0/350
2FGL J1846.6–2519											
J184700.67–245940.2	1215.87	1.19	0.11	2.75	0.1	2.13	0.28	0.12	0.19	C	2/5081
2FGL J1847.2–0236											
J184633.39–023728.2	613.36	0.69	0.04	2.28	0.08	1.47	0.3	0.25	0.12	B	0/1203
2FGL J1857.6+0211											
J185756.07+020729.2	323.88	0.58	0.05	2.1	0.07	1.98	0.22	0.3	0.07	B	0/415
2FGL J1901.1+0427											
J190055.36+041949.3	517.32	0.95	0.04	2.57	0.04	1.94	0.07	0.59	0.34	B	0/1306
2FGL J1902.7–7053											
J190317.61–705539.6	199.8	0.93	0.06	2.8	0.14	2.43	0.36	0.16	0.16	C	1/1056
2FGL J1904.8–0705											
J190444.57–070740.0	169.32	1.1	0.12	2.9	0.1	2.48	0.17	0.18	0.23	C	0/1562
2FGL J1914.0+1436											
J191415.95+142839.3	484.89	0.77	0.03	2.07	0.03	1.28	0.04	0.7	0.36	B	0/2020

Table 13: UGS Associations.

Name	distance (arcsec)	$c_{12}$	$\sigma_{12}$	$c_{23}$	$\sigma_{23}$	$c_{34}$	$\sigma_{34}$	$s_b$	$s_q$	class	$\pi$
2FGL J1917.0–3027											
J191637.70–303356.6	525.92	1.19	0.06	3.01	0.08	2.47	0.2	0.15	0.28	C	1/1040
2FGL J1923.4+2013											
J192142.39+201107.1	1491.67	1.08	0.12	2.61	0.07	2.29	0.13	0.28	0.27	B	7/14898
J192540.72+201244.2	1870.96	0.95	0.05	2.64	0.04	1.88	0.06	0.55	0.34	B	7/14898
J192501.65+204022.6	2080.26	0.95	0.06	2.28	0.04	2.01	0.08	0.43	0.22	B	7/14898
2FGL J1924.9–1036											
J192501.64–104315.3	409.6	1.36	0.07	3.31	0.06	2.65	0.09	0.00	0.4	B	0/1471
2FGL J1931.8+1325											
J193226.87+134708.5	1394.03	1.08	0.13	2.54	0.09	2.43	0.2	0.17	0.2	C	2/8391
2FGL J1936.5–0855											
J193635.53–091142.4	943.64	1.27	0.05	2.91	0.05	2.46	0.1	0.00	0.44	B	0/5385
J193718.37–090822.4	986.29	0.94	0.05	2.46	0.1	2.44	0.28	0.23	0.17	C	1/5385
2FGL J1944.3+7325											
J194738.74+732636.3	843.32	1.27	0.04	2.83	0.04	2.38	0.07	0.00	0.61	B	2/1991
J194312.51+731730.7	559.24	0.95	0.05	2.88	0.1	2.39	0.29	0.19	0.25	C	0/1991
2FGL J1947.8–0739											
J194757.07–075000.1	614.49	1.09	0.06	2.69	0.13	2.44	0.48	0.14	0.17	C	1/4369
2FGL J1949.7+2405											
J195012.96+235508.8	712.46	0.93	0.04	2.58	0.03	2.32	0.04	0.75	0.6	A	—
J195009.38+235610.2	634.3	0.61	0.04	2.13	0.04	1.45	0.12	0.41	0.18	B	—
J194857.53+240407.6	651.18	0.74	0.03	2.18	0.03	2.44	0.04	0.78	0.23	B	—
J194845.97+240237.4	820.79	0.79	0.05	2.12	0.06	2.19	0.08	0.47	0.00	B	—
2FGL J1950.3+1223											
J195014.42+123119.6	461.61	1.01	0.07	2.8	0.07	2.7	0.1	0.27	0.37	B	0/3119
2FGL J2006.2–0929											
J200802.67–093641.9	1617.39	0.81	0.05	2.75	0.1	2.4	0.24	0.19	0.14	C	2/15089
J200615.96–095721.0	1669.93	1.16	0.05	2.7	0.08	2.3	0.24	0.23	0.3	C	2/15089
J200728.94–090737.4	1688.58	1.24	0.06	2.82	0.1	2.31	0.28	0.12	0.25	C	2/15089
2FGL J2006.5–2256											
J200725.61–230605.9	906.51	1.05	0.05	2.91	0.09	2.39	0.21	0.28	0.29	B	0/2088
2FGL J2006.9–1734											
J200626.14–173418.6	429.99	1.04	0.05	2.78	0.08	2.37	0.24	0.28	0.29	B	0/2143
J200623.81–173639.2	473.07	1.16	0.07	3.09	0.11	2.73	0.23	0.13	0.24	C	0/2143

Table 14: UGS Associations.

Name	distance (arcsec)	$c_{12}$	$\sigma_{12}$	$c_{23}$	$\sigma_{23}$	$c_{34}$	$\sigma_{34}$	$s_b$	$s_q$	class	$\pi$
2FGL J2009.2–1505											
J200901.29–151620.3	700.87	1.02	0.06	3.02	0.1	2.52	0.24	0.17	0.26	C	0/1969
2FGL J2031.4–1842											
J203142.40–182208.0	1219.37	0.89	0.04	2.39	0.09	2.31	0.26	0.29	0.18	B	0/3790
J203159.63–183824.4	499.26	0.92	0.07	2.66	0.11	2.3	0.32	0.22	0.18	C	1/3790
J203003.91–184441.6	1208.58	1.23	0.06	2.85	0.12	2.43	0.32	0.11	0.23	C	1/3790
J203035.02–185910.1	1269.41	1.24	0.06	2.95	0.1	2.63	0.2	0.12	0.27	C	1/3790
2FGL J2044.4–4757											
J204444.65–481006.7	764.03	1.02	0.03	2.8	0.04	2.44	0.07	0.64	0.65	A	0/1279
J204520.57–475648.5	515.06	1.39	0.04	2.89	0.06	2.41	0.14	0.00	0.38	B	0/1279
2FGL J2131.0–5417											
J213014.80–540748.6	728.48	1.09	0.05	2.6	0.13	2.64	0.32	0.16	0.18	C	1/2080
2FGL J2200.1–6931											
J215916.12–692856.1	324.01	1.11	0.05	2.8	0.09	2.3	0.28	0.25	0.26	B	0/910